

Study of the interaction of sulfur dioxide derivative with cardiac sodium channel

Aifang Nie, Ziqiang Meng*

Institute of Environmental Medicine and Toxicology, Shanxi University, Taiyuan 030006, China

Received 20 August 2005; received in revised form 24 September 2005; accepted 30 September 2005

Available online 21 October 2005

Abstract

The effects of sulfur dioxide (SO₂) derivatives (bisulfite and sulfite, 1:3 M/M) on voltage-dependent sodium channel in isolated rat ventricular myocyte were studied using the whole cell patch-clamp technique. SO₂ derivatives increased sodium current (I_{Na}) in a concentration-dependent manner. SO₂ derivatives at 10 μ M significantly shifted steady-state inactivation curve of I_{Na} to more positive potentials, but did not affect the activation curve. SO₂ derivatives markedly shifted the curve of time-dependent recovery of I_{Na} from inactivation to the left, and accelerated the recovery of I_{Na} . SO₂ derivatives also significantly shortened the activation and inactivation time constants of I_{Na} . These results indicated that SO₂ derivatives produced concentration-dependent stimulation of cardiac sodium channels, which due mainly to the interaction of the drug with sodium channels in the inactivated state.

© 2005 Elsevier B.V. All rights reserved.

Keywords: Cardiomyocyte; Patch-clamp technique; Sodium channel; Sulfur dioxide

1. Introduction

SO₂ is a common air pollutant released into the atmosphere from the combustion of fossil fuel. Inhaled SO₂ can easily be hydrated to produce in the respiratory tract sulfurous acid, which subsequently dissociates to form its derivatives, bisulfite and sulfite (1:3 M/M, in neutral fluid) [1]. The derivatives can be absorbed into blood or other body fluid. In addition, bisulfite/sulfite enters the body via foods, beverages and drugs because sulfiting agents (sulfur dioxide, metabisulfite, bisulfite and sulfite) are widely used as preservatives [2]. Endogenous bisulfite/sulfite is generated during the normal processing of sulfur-containing amino acids [3] and also can be formed by the metabolism of sulfur-containing drugs, including *N*-acetylcysteine [4]. The natural SO₂ concentration is 0.04–0.45 mg/m³ in atmosphere. Epidemiological studies have linked SO₂ exposure with many respiratory diseases such as lung cancer [5] when SO₂ concentration exceeded 0.6 mg/m³. SO₂ inhalation may induce chromosomal aberrations (CA),

sister chromatid exchanges (SCE), and micronuclei (MN) in human peripheral blood lymphocytes. [2,6–8]. SO₂ inhalation may cause oxidation damage and DNA damage in various organs of mice and rat, especially in lung, heart and brains [9,10]. It indicated that SO₂ is a systemic toxicant [9]. In addition, SO₂ could affect the blood pressure of rat [11]. Therefore, SO₂ inhalation might have relation with cardiovascular diseases.

Over the past decade, many epidemiological studies have found associations between air pollution and many diseases. Recently, there is increased epidemiological evidence that SO₂ as a common air pollutant is associated with morbidity and mortality due to cardiovascular disease [12–15]. Many epidemiological studies in Asian cities (Hong Kong, Beijing, Shenyang, Taipei, Seoul et al.) demonstrated that SO₂ increased the risk of cardiovascular disease and the mortality due to cardiovascular disease [13,14,16,17]. Some studies indicated that SO₂ was associated with many kinds of cardiovascular disease, such as increasing the risk of developing a cardiac arrhythmia [18], ischemic heart diseases [19,20], pulmonary cardiac disease [21], affecting heart rate variability and blood pressure [12], etc.

Biological membranes are essential in maintaining cell integrity and function. Ion channels in cell membrane are

* Corresponding author. Tel./fax: +86 351 701 1895.

E-mail addresses: afnie@126.com (A. Nie),
zqmeng@sxu.edu.cn (Z. Meng).

targets for many toxins and drugs. Three prominent voltage-gated ion currents are expressed in cardiac ventricular muscle; the tetrodotoxin (TTX)-resistant sodium current (I_{Na}), the L-type calcium current ($I_{Ca,L}$) and the transient outward potassium current (I_{to}). These currents contribute in a precisely timed and regulated manner to the development, maintenance and termination of the action potential [22]. Voltage-gated sodium channels play a crucial role in regulating the electrical excitability of animal cells, being primarily responsible for the depolarization phase of the action potential [23].

Recently, we have found that the SO_2 derivatives affected sodium channels in the hippocampal CA1 neurons and dorsal root ganglion (DRG) neurons from rats [24–26]. However, little is known about the effects of SO_2 on sodium channel of mammalian cardiomyocytes. In the present study, we examined the effects of SO_2 derivatives on sodium channel in rat cardiomyocytes by using whole cell patch-clamp technique in order to probe into the possible mechanism of SO_2 on cardiovascular system.

2. Materials and methods

2.1. Isolation of single ventricular myocytes

Single ventricular myocytes were isolated from the heart of adult rats (200–300 g body weight, Wistar) by a modified enzymatic dissociation technique [27]. Rats were purchased from Experimental Animal Center of Shanxi Medical University (Grade II, Certificate No. 070101). All experiments conformed to local and international guidelines on ethical use of animals and all efforts were made to minimize the number of animal used and suffering. Briefly, the rats were stunned by heavy blow on the head. The heart was rapidly removed and placed in oxygenated ice-cold Ca^{2+} -free Tyrode's solution, and then the excised heart was mounted on a modified Langendorff apparatus for perfusion of the coronary arteries. Blood was removed by a 4-min period of perfusion with oxygenated 37 °C Tyrode's solution, which was followed by 5 min of perfusion with a nominally Ca^{2+} -free Tyrode's solution. Enzymatic digestion was initiated by 25 min of perfusion with 50 ml Ca^{2+} -free Tyrode's solution containing 15 mg collagenase (Type P, Boehringer Mannheim, Roche). At the end of enzyme perfusion, the heart was sequentially washed with 50 ml 0.2 mM Ca^{2+} Tyrode's solution plus 1 mg/ml bovine serum albumin. The ventricles were then cut off, chopped into small chunks and stirred in a small vessel containing 'Krafteburhe' (KB) solution until elongated, striated myocytes dissociated from the tissue pieces. Myocytes were harvested after filtering the cell-containing suspension through a nylon mesh (200 μ m). They were washed three times in storage solution and then maintained at room temperature in KB solution for at least 1 h before the electrophysiological experiment. The concentration of Ca^{2+} in Tyrode's solution was gradually increased to 1.8 mmol/L. All experiments were performed within 12 h after isolation.

2.2. Electrophysiological measurements

Isolated ventricular myocytes were placed in the experimental chamber mounted on the stage of an inverted microscope (Olympus, Japan). After setting to the bottom of chamber, the cells were superfused with the external solution containing for 10 min at a rate of 2–3 ml/min at 25 °C. Sodium currents were recorded with an Axopatch 200B patch clamp amplifier (Axon Instruments, Foster City, CA, USA). Glass microelectrodes were made using a micropipette puller (PP 830, Narishige, Japan) and had a resistance of 1–2 M Ω , when filled with electrode internal solution. Only the rod shaped cells with visible striations were used for experiments. Liquid junction potential between the pipette solution and external solution was corrected after the pipette tipped into the external solution. After forming a conventional "gigaseal", the membrane was ruptured with a gentle suction to obtain the whole cell voltage-

clamp configuration. To minimize the duration of capacitive current, membrane capacitance and series resistance were compensated after membrane rupture. K^+ current was suppressed by substituting intracellular K^+ by Cs^+ . Ca^{2+} currents were blocked by adding $CdCl_2$ in the external solution before the electrophysiological recording. Evoked currents were low-pass filtered at 2 kHz, digitized at 10 kHz, command pulses were generated by a Digidata 1200B (Axon) controlled by pCLAMP version 6.0.4 software (Axon Instruments, CA, USA), and on-line acquired data stored in a PC486 computer for subsequent analysis. All experiments were carried out at room temperature (22–24 °C) 3 to 12 h after isolation of rat cardiomyocytes.

2.3. Solutions

Tyrode's solution contained (in mM): NaCl 137, KCl 5, $MgCl_2$ 1, NaH_2PO_4 0.33, $CaCl_2$ 1.8, HEPES 10, Glucose 10, pH 7.4. KB solution contained (in mM): L-Glu 50, KCl 30, Tau 20, KH_2PO_4 30, $MgCl_2$ 1, HEPES 10, Glucose 10, EGTA 0.5, pH 7.4. The external solution containing (in mM): NaCl 5, CsCl 135, $MgCl_2$ 1, $CaCl_2$ 2, HEPES 10, Glucose 10, pH 7.4. The electrode internal solution containing (in mM): CsCl 130, NaCl 5, HEPES 5, EGTA 5, MgATP 5, $MgCl_2$ 1, pH 7.2.

2.4. Drug application and data analysis

For drug application, a series of microtubes (200 μ m i.d.) were glued together side by side. Solutions were fed from independent reservoirs by gravity. The micro-tubes were shifted horizontally with a mini-manipulator for aligning the flow of solution from the tubes relative to the cell. By this system, we can rapidly change the extracellular solution surrounding the myocyte and test the effects of drugs in different concentration on the same cell. This method is similar to that used by Xu et al. [28]. Sodium sulfite and sodium bisulfite

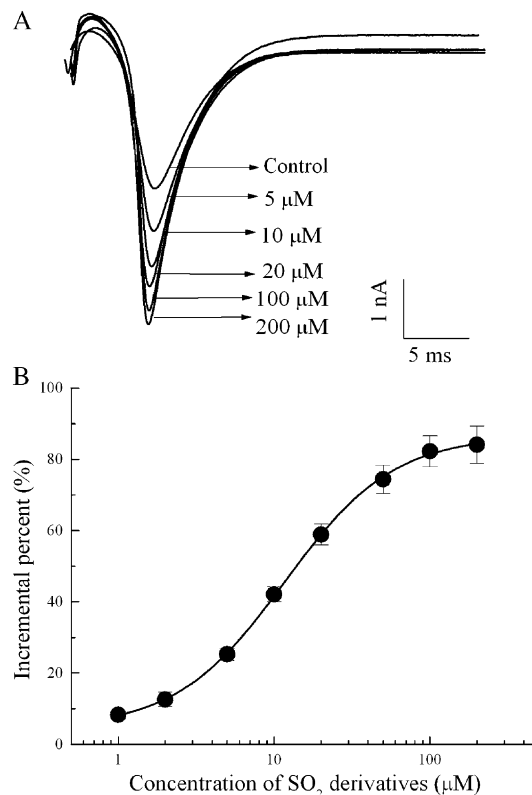


Fig. 1. SO_2 derivatives enhanced voltage-gated cardiac sodium currents in a concentration-dependent manner. (A) Traces of I_{Na} evoked in the absence and presence of SO_2 derivatives. Currents were elicited by depolarization from a HP of -80 mV to -40 mV. (B) Concentration–response curve of the SO_2 derivatives enhancement on I_{Na} . Each point represents mean \pm S.D. ($n=8$).

were purchased from Sigma and dissolved in the extracellular solution as 3:1 molar ratio.

All data were analyzed by the use of pCLAMP 6.0 and Origin 5.0 software (Microcal software, USA). All values were presented as mean \pm S.D., and statistical comparisons were made using the paired Student's *t* test and one-way ANOVA procedure, and the probabilities less than 0.05 were considered significant.

3. Results

3.1. SO_2 derivatives increased I_{Na} in a concentration-dependent manner

Cardiac myocytes were held at a holding potential (HP) of -80 mV, an inward current was recorded with 30-ms voltage steps to between -70 and $+40$ mV from a HP of -80 mV with 10 mV increment. The inward current was reversibly blocked by $1 \mu\text{M}$ TTX, indicating that current were attributed to sodium current.

Upon the application of SO_2 derivatives, the amplitudes of I_{Na} were increased, and this action progressed with increment in concentrations from 1 to 200 μM (Fig. 1A, B). Under the control conditions, the currents were decreased by $5.36 \pm 0.5\%$ ($n=8$). The peak amplitude of I_{Na} was increased by $8.3 \pm 1.1\%$

and $84.1 \pm 5.3\%$ ($n=8$) with SO_2 derivatives at 1 μM and 200 μM , respectively (Fig. 1B). Concentration–response curve was obtained by plotting the incremental percent against the concentration of SO_2 derivatives, and the curve was fitted with the Hill function (Eq. (1)):

$$E = E_{\text{max}} / [1 + (\text{EC}_{50}/C)^n] \quad (1)$$

where E is the percent of the increase of I_{Na} , E_{max} is the maximal percent of the increase of I_{Na} , the EC_{50} is the concentration of SO_2 derivatives for half-maximum increase, C is the concentration of SO_2 derivatives, and n , the Hill coefficient. The EC_{50} of SO_2 derivatives on I_{Na} was $10.97 \pm 0.61 \mu\text{M}$, with n of 1.07 ± 0.05 . The effect of the drug was poorly reversible after washout. The result indicated that the effect of SO_2 derivatives on I_{Na} is concentration dependent.

3.2. Effect of SO_2 derivatives on voltage-dependent activation of I_{Na}

To test the effect of SO_2 derivatives on I_{Na} steady-state activation, sodium currents were evoked by a series of 10-mV

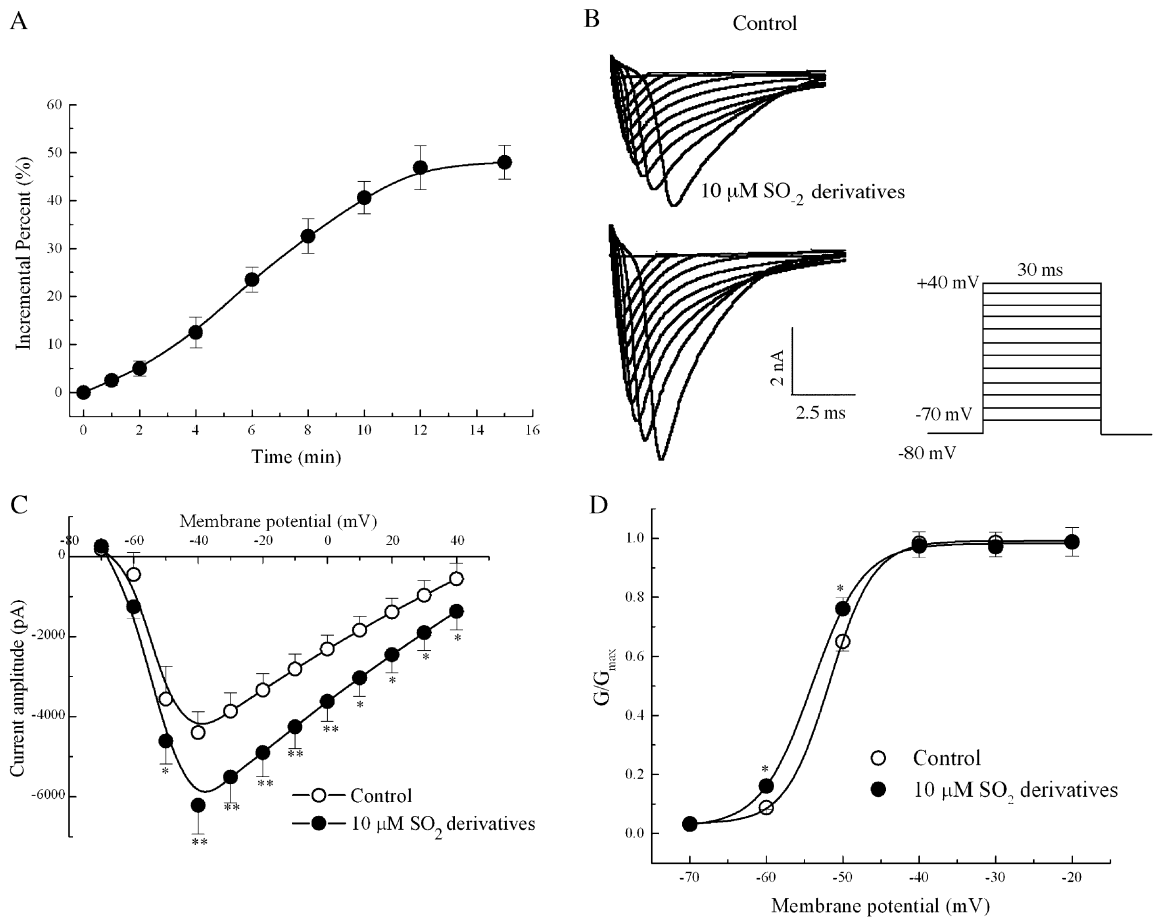


Fig. 2. Effects of SO_2 derivatives on the activation of I_{Na} . (A) Time course of the enhancement of SO_2 derivatives on I_{Na} . (B) Superimposed current traces in the absence (top traces) and presence (bottom traces) of 10 μM SO_2 derivatives were evoked by 30-ms pulses from -70 to $+40$ mV with 10 mV increments every 2 s (see inset). The holding membrane potential was set at -80 mV. (C) Current–voltage (I – V) relationships in the absence (○) and presence (●) of 10 μM SO_2 derivatives were plotted according to the amplitudes of peak I_{Na} elicited by the voltage protocol in the panel B. (D) Activation curves of I_{Na} in the absence (○) and presence (●) of 10 μM SO_2 derivatives. The data were well fitted by Boltzmann equation. Each point represents mean \pm S.D. ($n=8$) * $P<0.05$, ** $P<0.01$ vs. control.

voltage steps to potentials between -70 and $+40$ mV from a holding potential of -80 mV. In the experiments where 30-ms test pulses were applied, currents were measured at their peaks. Representative recorded traces before and after application of $10\ \mu\text{M}$ SO_2 derivatives are shown in Fig. 2B. The enhancement effect of SO_2 derivatives on I_{Na} is increased steadily over 10 min (Fig. 2A). Current–voltage (I – V) curves for I_{Na} before and after application of $10\ \mu\text{M}$ SO_2 derivatives were constructed by plotting the peak of the whole cell current against the test potentials. As shown in Fig. 2C, the threshold for activation of I_{Na} was approximately -60 mV and the peak amplitude of I_{Na} was approximately at -40 mV.

In order to quantify the effect of SO_2 derivatives on the channel activation, G – V curves were constructed (Fig. 2D). The curves were drawn according to the Boltzmann equation (Eq. (2)):

$$G/G_{\text{max}} = 1/1 + \exp[-(V - V_h)/k], \quad (2)$$

where G is conductance, G_{max} is maximum conductance, V is the membrane potential, V_h is the voltage at which half-maximal effect is obtained, and k is the slope factor. Conductance was calculated by using the equation (Eq. (3)):

$$G = I/(V - V_{\text{Na}}), \quad (3)$$

where I is current amplitude and V_{Na} is the reversal potential (V_{Na} was estimated by extrapolation from the steep linear ascending part of the I – V relation to the zero-current axis). SO_2 derivatives shifted G – V curve of sodium current toward the hyperpolarizing direction. The values of V_h for activation of I_{Na} in control and in the presence of $10\ \mu\text{M}$ SO_2 derivatives were -51.72 ± 0.15 mV ($n=8$) and -54.03 ± 0.21 mV ($n=8$, $P>0.05$), with k of 2.88 ± 0.17 mV ($n=8$) and 3.33 ± 0.15 mV ($n=8$, $P>0.05$), respectively. The SO_2 derivatives-induced shift of V_h was not statistically significant.

3.3. Effect of SO_2 derivatives on steady-state inactivation of I_{Na}

Fig. 3A shows the effect of SO_2 derivatives on the voltage-dependence of I_{Na} inactivation using a double-pulse protocol (see inset): the membrane was first stepped to potentials between -120 and -20 mV to condition I_{Na} and then -10 mV to test the extent of inactivation. A selected I_{Na} inactivation traces from a typical experiments are shown in Fig. 3A. The inactivation curves shown in Fig. 3B were obtained by plotting the normalized I_{Na} against the prepulse voltages. The plots were well fitted with a single Boltzmann function (Eq. (4)):

$$I/I_{\text{max}} = 1/1 + \exp[(V - V_h)/k], \quad (4)$$

where V is the prepulse potential, V_h is the potential where normalized I was reduced to one half and k is the slope factor. SO_2 derivatives ($10\ \mu\text{M}$) caused a positive shift of the inactivation curve along the potential axis [control $V_h = -76.04 \pm 0.49$ mV vs. SO_2 derivatives -69.63 ± 0.49 mV ($n=8$, $P<0.05$)]. However, the slope factor k [control

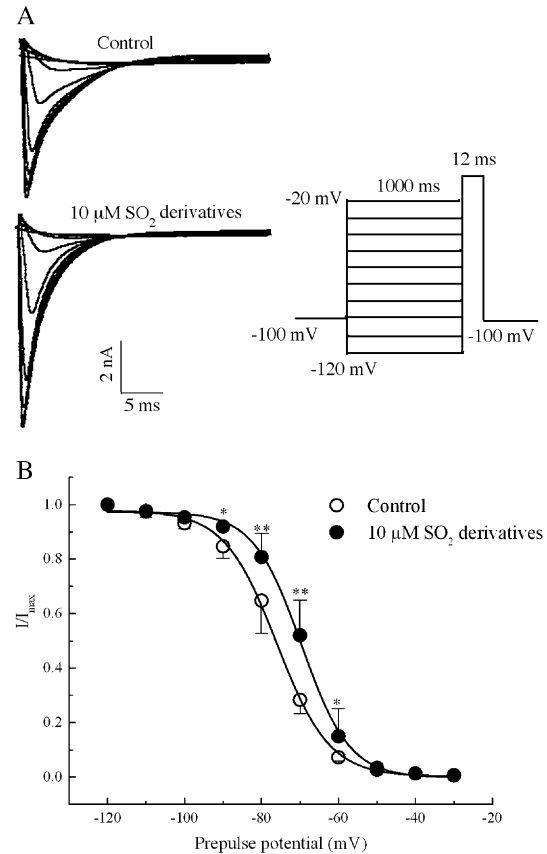


Fig. 3. Effect of SO_2 derivatives on steady-state inactivation of I_{Na} . (A) Inactivation current traces in control (top traces) and $10\ \mu\text{M}$ SO_2 derivatives treated (bottom traces) examined with a double-pulse protocol (see inset). (B) Normalized steady-state inactivation of I_{Na} in the absence (○) and presence of $10\ \mu\text{M}$ derivatives (●) were plotted as a function of the conditioning voltages. The steady-state inactivation curves were fitted with Boltzmann function (see text). The value of each point is mean \pm S.D. ($n=8$) * $P<0.05$, ** $P<0.01$ vs. control.

6.83 ± 0.44 mV vs. SO_2 derivatives 6.21 ± 0.44 mV ($n=8$, $P>0.05$)] remained unchanged.

3.4. Effect of SO_2 derivatives on recovery of I_{Na} from inactivation

The kinetics of recovery of I_{Na} from inactivation in the absence and presence of SO_2 derivatives were evaluated by identical two-pulse protocols (Fig. 4A, inset). To inactivate cardiac sodium channels, we applied a 100 ms prepulse to -30 mV from a holding potential of -80 mV. This fixed prepulse was followed by a return to HP with variable duration (Δt) and then by a 100-ms test pulse to -30 mV. The time course of recovery from inactivation of I_{Na} was fitted well with a bi-exponential function (Fig. 4B, open circle). Under control condition, the fast (τ_f) and slow (τ_s) recovery time constants of I_{Na} were 54.8 ± 4.3 ms and 144.3 ± 6.3 ms ($n=8$). In the presence of $10\ \mu\text{M}$ SO_2 derivatives, the recovery from inactivation of I_{Na} also was fitted well with a two-exponential function (Fig. 4B, solid circle) with the values of 49.6 ± 3.6 ms for τ_f and 109.2 ± 5.2 ms for τ_s ($n=8$). The difference of slow recovery time constant between control and SO_2 derivatives are

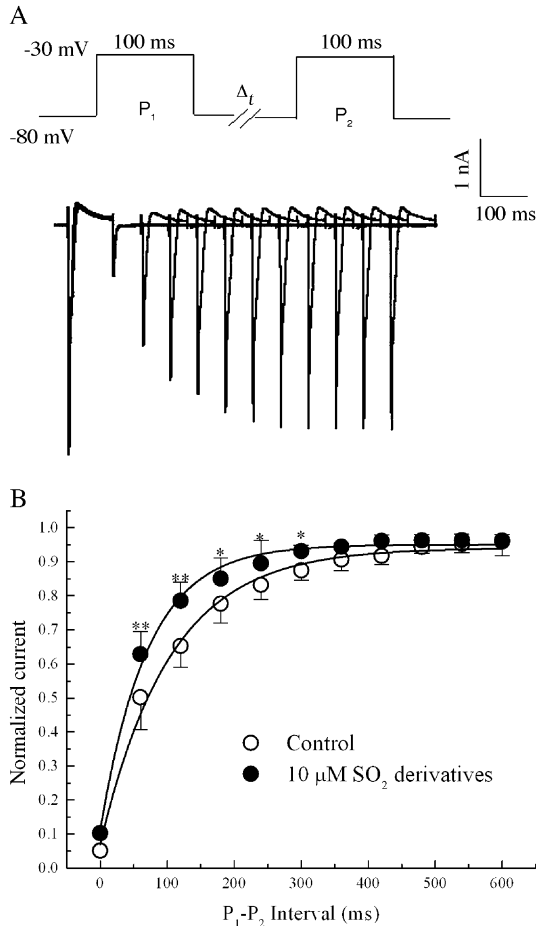


Fig. 4. Effect of SO_2 derivatives on kinetics of recovery of I_{Na} from inactivation. (A) Superimposed current traces for recovery of I_{Na} from inactivation. The pulse protocol was composed of two pulses, one 100-ms prepulse from -80 to -30 mV, followed by a depolarizing pulse to -80 mV with progressively prolonged durations from 0 to 600 ms and then a 100-ms test pulse to -30 mV. The membrane holding potential was -80 mV and the rate of pulse was 0.5 Hz. (B) The time course of recovery of peak I_{Na} from inactivation is shown in the absence (○) and presence of $10 \mu\text{M}$ SO_2 derivatives (●). Currents were normalized to their maximal values of I_{Na} recorded before application of the protocol. Recovery of I_{Na} from inactivation was markedly accelerated for τ_s in the presence of $10 \mu\text{M}$ SO_2 derivatives. Data were fitted well with two-exponential function. The value of each point is mean \pm S.D. ($n=8$) * $P<0.05$, ** $P<0.01$ vs. control.

significant ($P<0.05$, $n=8$). These results indicated that SO_2 derivatives accelerated recovery from inactivation of cardiac sodium channels.

3.5. Effect of SO_2 derivatives on kinetics of I_{Na} activation and inactivation

The records in Fig. 2B show that the kinetics of I_{Na} activation and inactivation are more rapid in presence of SO_2 derivatives than in absence. The differences in kinetics are highlighted in Fig. 5, where the I_{Na} recordings were for steps to -40 mV in control (left panel) and $10 \mu\text{M}$ SO_2 derivatives (right panel). The kinetics of both I_{Na} activation and inactivation could be well fitted by mono-exponential functions. Fig. 5B, C show that the mean time constants for activation (τ_m) and inactivation (τ_h) are significantly greater

($P<0.05$ or $P<0.01$) in control than in presence of $10 \mu\text{M}$ SO_2 derivatives over the entire range investigated (from -40 to $+40$ mV). At -40 mV, τ_m of I_{Na} was 0.91 ± 0.24 ms in control, and 0.81 ± 0.13 ms in the presence of $10 \mu\text{M}$ SO_2 derivatives, whereas τ_h of I_{Na} was 3.82 ± 0.52 ms in control, and 3.10 ± 0.63 ms in the presence of $10 \mu\text{M}$ SO_2 derivatives ($P<0.05$). These results indicated that SO_2 derivatives shortened the time constants for both activation and inactivation of I_{Na} , but it only significantly affected the inactivation time constant and the effect on the activation time constant was slightly.

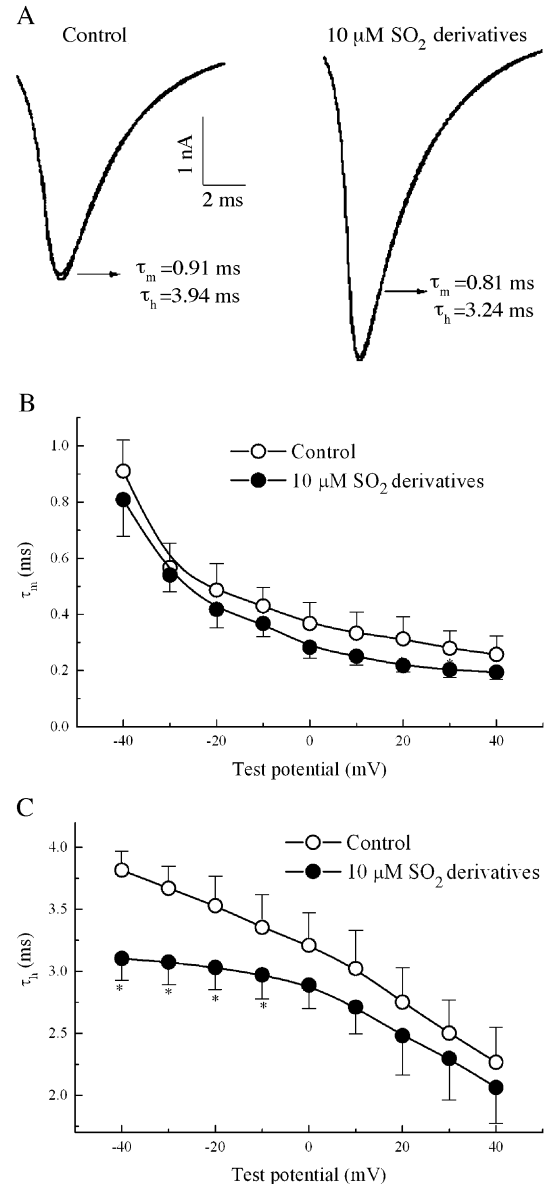


Fig. 5. Effects of SO_2 derivatives on kinetics of time dependent activation and inactivation of I_{Na} in rat ventricular myocytes. (A) Current traces elicited by a 30-ms voltage step to -40 mV from -80 mV in control and SO_2 derivatives. The raw data were fitted by mono-exponential function with activation (τ_m) and inactivation (τ_h) time constants shown. (B) and (C) Voltage-dependence of activation (τ_m) and inactivation (τ_h) time constants of I_{Na} under the control (○) and $10 \mu\text{M}$ SO_2 derivatives treated (●). Both τ_m and τ_h were smaller after application of $10 \mu\text{M}$ SO_2 derivatives. The value of each point is mean \pm S.D. ($n=8$) * $P<0.05$, ** $P<0.01$ vs. control.

4. Discussion

This study has shown that SO_2 derivatives significantly enhanced voltage-gated sodium channels (VGSC) in a concentration-dependent manner in isolated adult rat cardiomyocytes. The data obtained in the experiments demonstrated for the first time that SO_2 derivatives stimulated I_{Na} in mammalian cardiac myocytes. Stimulation of the I_{Na} by SO_2 derivatives in our study was concentration-dependent and irreversible. Most of the observed current increases were due to the increase in the maximum conductance. A minor part can be explained by changes in voltage-dependent parameters. In the present experiments, SO_2 derivatives increased I_{Na} and its EC_{50} value was approximate 10 μM .

SO_2 derivatives (10 μM) significantly shifted the inactivation curve to more positive potentials (V_h from -76 to -69 mV), but shifted the activation curve to negative potentials (V_h from -52 to -54 mV) and this effect was not significant. These results showed that SO_2 derivatives mainly affected the inactivation course of cardiac sodium channels. The positive shift in the steady-state inactivation curve might contribute to the increase of I_{Na} . SO_2 derivatives at 10 μM shortened both the fast and slow components of recovery from inactivation of cardiac sodium channels, but the effect on slow time constant was significant (from 144.3 to 109.2 ms). In addition, SO_2 derivatives also shortened both the activation and inactivation time constants of cardiac sodium channels, but the effect on the latter was significant. These results also indicated that SO_2 derivatives mainly interacted with the inactivation state of sodium channels.

Cardiac sodium channels play a critical role in the initiation and propagation of the cardiac action potential [29]. The fundamental properties that enable sodium channels to carry out their physiological roles include rapid, voltage-dependent activation, which opens the channel, and inactivation closes the channel and prevents it from reopening until there has been sufficient time for recovery. Many toxins, insecticides, and clinically useful drugs affect sodium channel inactivation [23].

The past studies in our laboratory have showed that SO_2 derivatives modulated sodium channels in DRG neurons [24] and hippocampal CA1 neurons [25,26]. SO_2 derivatives mainly affected the inactivation course of sodium channels in two neurons above mentioned. In the present study, SO_2 derivatives at the same concentration also mainly affected the inactivation of cardiac sodium channels. All these data suggested that SO_2 derivatives modulation of sodium channels was not specific on cell types or channel isoforms.

The mechanism by which SO_2 derivatives affect cardiac sodium channels are not clear now. However, we hypothesize that there are several potential interpretations. One possibility is that SO_2 derivatives affect the redox state of sodium channels. It has been shown that membrane proteins, including ion channels, are responsive to redox state [30]. Changes in the redox state of amino acid residues in channel proteins may lead to a conformational change and alterations of channel activity [31]. SO_2 dissolved in body fluid and

form its derivatives, sulfite and bisulfite. The one-electron oxidation of bisulfite produces the sulfur trioxide radical anion, which reacts rapidly with molecular oxygen to form a peroxy radical, and further forms several kinds sulfur- and oxygen-centered free radicals, such as $\text{SO}_3^{\cdot-}$, $\text{SO}_4^{\cdot-}$, and $\text{SO}_5^{\cdot-}$ etc [32,33]. The free radicals generated by SO_2 can damage nucleic acids [7,34] and induce mutation [7,35,36]. Moreover, these radicals can react with proteins and lipids [37]. It is possible that SO_2 derivatives can induce a change in redox state of amino acid residues of sodium channel proteins, leading to a conformational change and subsequently an alteration of the channel properties. Our previous study indicated that three kinds of antioxidase (SOD, CAT, Gpx) could partly inhibit the enhancement effect of SO_2 and sulfite on sodium channel of rat hippocampal neurons [26]. Therefore, the detailed mechanism of the sulfite, bisulfite-induced sodium current enhancement may involve the formation of sulfur- and oxygen-centered free radicals. These radicals might react with sodium channel protein and cause several kinds of electrophysiological changes, like as the changes in the present study. Another possible mechanism might involve the changes in intracellular signaling pathways. Previous studies have indicated that sodium channels be involved in signal transduction in neurons and cardiac myocytes [38]. Some drugs could regulate the activity of sodium channels through G-protein linked second-messenger systems [39]. Our recent study suggested that SO_2 derivatives might modulate L-type calcium channel via cAMP-PKA pathway [40]. Therefore, SO_2 derivatives might enhance sodium channels through mobilization of some common second messenger. The specific mechanism of SO_2 derivatives affecting sodium channel should be studied further in detail.

In summary, the results of the present work suggested that SO_2 derivatives could modulate voltage-gated sodium channels in rat cardiac myocytes. This modulation involved an increase of peak I_{Na} with a change in the voltage dependence inactivation and activation of I_{Na} , the acceleration of the time course of the activation, inactivation and the recovery from inactivation, which might lead to cardiac abnormalities, result in arrhythmias and frequently in sudden cardiac death. Hence, our study suggested that inhalation SO_2 or intake food containing sulfite (bisulfite, metabisulfite, etc) might also increase the cardiac contractility or cause several kinds of cardiomyopathies.

Acknowledgements

This study was supported by Grant No.30230310 from the National Natural Science Foundation of China and by a Grant No.20031092 from the National Natural Science Foundation of Shanxi Province.

References

- [1] R. Shapiro, Genetic effects of bisulfite (sulfur dioxide), *Mutat. Res.* 39 (1977) 149–175.

- [2] E. Rencüzoğullari, H.B. İla, A. Kayraldiz, A.M. Top, Chromosome aberrations and sister chromatid exchanges in cultured human lymphocytes treated with sodium metabisulfite, a food preservative, *Mutat. Res.* 490 (2001) 107–112.
- [3] T. Ubuka, S. Yuasa, J. Ohta, N. Masuoka, K. Yao, M. Kinuta, Formation of sulfate from L-cysteine in rat liver mitochondria, *Acta Med. Okayama* 44 (1990) 55–64.
- [4] I.A. Cotgreave, M. Berggren, T.W. Jones, J. Dawson, P. Moldeus, Gastrointestinal metabolism of N-acetylcysteine in the rat, including an assay for sulfite in biological systems, *Biopharm. Drug Dispos.* 8 (1987) 377–386.
- [5] D.A. Atkinson, T.C. Sim, J.A. Grant, Sodium metabisulfite and SO₂ release: an under-recognized hazard among shrimp fishermen, *Ann. Allergy* 71 (1993) 563–566.
- [6] Z. Meng, N. Sang, B. Zhang, Effects of derivatives of sulfur dioxide on micronuclei formation in mouse bone marrow cells in vivo, *Bull. Environ. Contam. Toxicol.* 69 (2002) 257–264.
- [7] Z. Meng, B. Zhang, Polymerase chain reaction based deletion screening of bisulfite (sulfur dioxide)-enhanced gpt mutants in CHO-AS52 cells, *Mutat. Res.* 425 (1999) 81–85.
- [8] Z. Meng, L. Zhang, Cytogenetic damage induced in human lymphocytes by sodium bisulfite, *Mutat. Res.* 298 (1992) 63–69.
- [9] Z. Meng, Oxidative damage of sulfur dioxide on various organs of mice: sulfur dioxide is a system oxidative damage agent, *Inhal. Toxicol.* 15 (2003) 181–195.
- [10] Z. Meng, G. Qin, B. Zhang, J. Bai, DNA damaging effects of sulfur dioxide derivatives in cells from various organs of mice, *Mutagenesis* 19 (2004) 465–468.
- [11] Z. Meng, H. Geng, J. Bai, G. Yan, Blood pressure of rats lowered by sulfur dioxide and its derivatives, *Inhal. Toxicol.* 15 (2003) 951–959.
- [12] U. de Paula Santos, A.L. Braga, D.M. Giorgi, L.A. Pereira, C.J. Grupi, C.A. Lin, M.A. Bussacos, D.M. Zanetta, P.H. do Nascimento Saldiva, M.T. Filho, Effects of air pollution on blood pressure and heart rate variability: a panel study of vehicular traffic controllers in the city of Sao Paulo, Brazil, *Eur. Heart J.* 26 (2005) 193–200.
- [13] C.C. Changa, S.S. Tsaib, S.C. Hoa, C.Y. Yanga, Air pollution and hospital admissions for cardiovascular disease in Taipei, Taiwan, *Environ. Res.* 98 (2005) 114–119.
- [14] T.W. Wong, W.S. Tam, T.S. Yu, A.H. Wong, Associations between daily mortalities from respiratory and cardiovascular diseases and air pollution in Hong Kong, China, *Occup. Environ. Med.* 59 (2002) 30–35.
- [15] T.W. Wong, T.S. Lau, T.S. Yu, A. Neller, S.L. Wong, W. Tam, S.W. Pang, Air pollution and hospital admissions for respiratory and cardiovascular diseases in Hong Kong, *Occup. Environ. Med.* 56 (1999) 679–683.
- [16] G. Chang, X. Pan, X. Xie, Y. Gao, Time-series analysis on the relationship between air pollution and daily mortality in Beijing, *Wei Sheng Yan Jiu* 6 (2003) 565–568.
- [17] Z. Xu, D. Yu, L. Jing, X. Xu, Air pollution and daily mortality in Shenyang, China, *Arch. Environ. Health* 55 (2000) 115–120.
- [18] S. Vedal, K. Rich, M. Brauer, R. White, J. Petkau, Air pollution and cardiac arrhythmias in patients with implantable cardioverter defibrillators, *Inhal. Toxicol.* 16 (2004) 353–362.
- [19] K. Toren, S. Hagberg, H. Westberg, Health effects of working in pulp and paper mills: exposure, obstructive airways diseases, hypersensitivity reactions, and cardiovascular diseases, *Am. J. Ind. Med.* 29 (1996) 111–122.
- [20] G. Ciccone, F. Faggiano, P. Falasca, SO₂ air pollution and hospital admissions in Ravenna: a case-control study, *Epidemiol. Prev.* 19 (1995) 99–104.
- [21] X. Xu, J. Gao, D.W. Dockery, Y. Chen, Air pollution and daily mortality in residential areas of Beijing, China, *Arch. Environ. Health* 49 (1994) 216–222.
- [22] K.B. Walsh, G.E. Parks, Changes in cardiac myocyte morphology alter the properties of voltage-gated ion channels, *Cardiovasc. Res.* 55 (2002) 64–75.
- [23] A.L. Goldin, Mechanisms of sodium channel inactivation, *Curr. Opin. Neurobiol.* 13 (2003) 284–290.
- [24] Z. Du, Z. Meng, Modulation of sodium currents in rat dorsal root ganglion neurons by sulfur dioxide derivatives, *Brain Res.* 1010 (2004) 127–133.
- [25] Z. Meng, N. Sang, Effect of SO₂ derivatives on sodium currents in acutely isolated rat hippocampal CA1 neurons, *Acta Physiol. Sin.* 54 (2002) 267–270.
- [26] Z. Meng, A. Nie, Enhancement of sodium metabisulfite on sodium currents in acutely isolated rat hippocampal CA1 neurons, *Environ. Toxicol. Pharmacol.* 20 (2005) 35–41.
- [27] G. Isenberg, U. Klöckner, Calcium tolerant ventricular myocytes prepared by preincubation in a “KB medium”, *Pflügers Arch.* 395 (1982) 6–18.
- [28] T. Xu, N.J. Liu, C.Q. Li, Y. Shanguan, Y.X. Yu, H.G. Kang, J.S. Han, Cholecystokinin octapeptide reverses the k-opioid-receptor-mediated depression of calcium current in rat dorsal root ganglion neurons, *Brain Res.* 730 (1996) 207–211.
- [29] G.R. Li, C.P. Lau, A. Shrier, Heterogeneity of sodium current in atrial vs epicardial ventricular myocytes of adult guinea pig hearts, *J. Mol. Cell. Cardiol.* 34 (2002) 1185–1194.
- [30] A. Bertl, C.L. Slayman, Cation-selective channels in the vacuolar membrane of *Saccharomyces*: dependence on calcium, redox state, and voltage, *Proc. Natl. Acad. Sci. U. S. A.* 87 (1990) 7824–7828.
- [31] J.P. Ruppersberg, M. Stocker, O. Pongs, S.H. Heinemann, R. Frank, M. Koenen, Regulation of fast inactivation of cloned mammalian *Ik(A)* channels by cysteine oxidation, *Nature* 352 (1991) 711–714.
- [32] X. Shi, Generation of SO₃^{•−} and OH^{•−} radicals in SO₃^{2−} reactions with inorganic environmental pollutants and its implications to SO₃^{2−} toxicity, *J. Inorg. Biochem.* 56 (1994) 155–165.
- [33] X. Shi, Y. Mao, 8-Hydroxy-2'-deoxyguanosine formation and DNA damage induced by sulfur trioxide anion radicals, *Biochem. Biophys. Res. Commun.* 205 (1994) 141–147.
- [34] H. Hayatsu, R.C. Miller, The cleavage of DNA by the oxygen-dependent reaction of bisulfite, *Biochem. Biophys. Res. Commun.* 46 (1972) 120–124.
- [35] H. Hayatsu, A. Miura, The mutagenic action of sodium bisulfite, *Biochem. Biophys. Res. Commun.* 39 (1970) 156–160.
- [36] D.A. Pagano, E. Zeiger, A.A. Stark, Autoxidation and mutagenicity of sodium bisulfite, *Mutat. Res.* 228 (1990) 89–96.
- [37] M. Reist, P. Jenner, B. Halliwell, Sulphite enhances peroxynitrite-dependent α 1-antiproteinase inactivation: a mechanism of lung injury by sulphur dioxide? *FEBS Lett.* 423 (1998) 231–234.
- [38] R.A. Nicholson, C. Liao, J. Zheng, L.S. David, L. Coyne, A.C. Errington, G. Singh, G. Lees, Sodium channel inhibition by anandamide and synthetic cannabimimetics in brain, *Brain Res.* 978 (2003) 194–204.
- [39] R.F. Lundy Jr., Potential mechanisms for functional changes in taste receptor cells following sodium deficiency in mammals, *Neurosci. Biobehav. Rev.* 23 (1998) 103–109.
- [40] A. Nie, Z. Meng, Modulation of L-type calcium current in rat cardiac myocytes by sulfur dioxide derivatives, *Food Chem. Toxicol.* (2005).